

Chunfang Wei · Louise S. Lintilhac
Philip M. Lintilhac

Loss of stability, pH, and the anisotropic extensibility of *Chara* cell walls

Received: 10 May 2005 / Accepted: 3 October 2005 / Published online: 12 November 2005
© Springer-Verlag 2005

Abstract We investigated the effects of acid conditions on the extensibility of isolated wall segments from growing *Chara corallina* cells, providing the first detailed multi-azimuthal description of the anisotropic elastic modulus of the walls. The values of anisotropic modulus were obtained by loading a tensile force on wall ribbons excised from the cell walls along twelve different azimuths, and measuring the resulting elongation of the ribbons. Our study differs from previous studies in which mechanical loading of the wall materials was performed under creep conditions. We used ramp-loading conditions which meet the requirements for *Loss of Stability*. The results show that whereas a linear relationship between wall extension and log time is typical for creep-based experiments, it is not seen under ramp-loading conditions. To clarify the relative values of the wall moduli, the complete all-around anisotropic modulus is presented in polar coordinates, with the value of longitudinal modulus normalized to one unit. Acid pH enhances the extensibility of the wall materials, especially when medium $\text{pH} \leq 4$, indicating that it is necessary to eliminate the prolonged plastic extension in order to obtain meaningful modulus values of wall materials immersed in acid environments.

Keywords Chara · Elastic modulus · Anisotropy · Creep · Loss of stability

Introduction

The anisotropic mechanical properties of plant cell walls have long been studied as a means of probing wall behavior during cell expansion. Much of the work has been carried out using the internodal cells of *Nitella* or *Chara* because they do not need to be isolated from a multicellular tissue and can be easily studied as individual cells. Moreover, the cells are so large that the walls can be cut into ribbons whose physical features can be measured with relative ease. Mechanical testing for wall anisotropy is usually performed under uniaxial loading conditions because it is convenient and capable of revealing the directionalities of wall properties, even though in vivo wall stress arises from cell turgor pressure which results in multiaxial loading. Previous studies on wall anisotropy have focused on revealing the longitudinal and transverse moduli. The modulus values along other directions have not yet been worked out. In this paper we present a detailed azimuthal assessment of wall modulus of growing *Chara corallina* cells.

Plant cell wall anisotropy was first demonstrated by Probine and Preston (1961) by means of dimensional investigation on the swelling of isolated wall segments in water. They opened *Nitella opaca* cells out flat, dried them down onto a glass plate, and measured the dimensions of the walls using microscopy and a displacement transducer. A drop of water was then placed on the wall specimen and, after swelling had ceased, they re-measured the dimensions. They found that in the transverse direction the increase in dimension was of the order of 4%, whereas in the longitudinal direction it was about 6%. This result showed for the first time the anisotropic nature of the cell walls. In a further attempt to understand the role that wall elasticity plays in the control of cell growth, Probine and Preston (1962) applied a tensile load to the wall specimen. A rectangular *Nitella opaca* wall ribbon cut either parallel or perpendicular to the cell axis was mounted on a loading/unloading apparatus. They found that under the same

C. Wei (✉) · P. M. Lintilhac
Department of Botany, University of Vermont,
Burlington, VT 05405, USA
E-mail: Chunfang.Wei@uvm.edu

C. Wei
Department of Physics, Guangxi National University,
Guangxi 530006, China

L. S. Lintilhac
Middlebury College, Middlebury, VT 05753, USA

stress level the strains of the two ribbons were not the same, indicating that the longitudinal modulus was different from the transverse modulus. Furthermore, they revealed that the degree of anisotropy varied with the growth rate of the cells, i.e., fast growing cells were more stretchy in the longitudinal direction relative to the transverse direction.

The transverse and longitudinal elastic properties of *Nitella axillaris* were also investigated by Métraux and Taiz (1978). In order to avoid the difficulty of gluing short transverse wall ribbons to the testing device, they measured the transverse modulus by hooking short wall sections (“wall loops”) into an extensometer. The results showed that in the transverse direction the cell walls exhibited a yield point whose value was approximately double that of longitudinal direction. This relationship held true for both young and old cells. Moreover, in young cells the longitudinal elastic extensibility was found to exceed the transverse extensibility by a factor of 4–7. These findings provided further direct evidence that transversely oriented cellulose microfibrils act as a “reinforcing filler” in the walls.

Acid pH has long been known to affect the elasticity of plant cell walls. The idea gave rise to the so-called Acid Growth Theory, which suggests that hydrogen ions promote wall-loosening, resulting in cell growth (Rayle and Cleland 1970; Cleland 1971; Hager et al. 1971; Rayle 1973; Métraux et al. 1980). Much support for the Acid Growth Theory comes from auxin-related experiments showing first, that auxin-treated growing tissues excrete protons, lowering the pH of the apoplast, and second, that treatment of auxin-sensitive tissues with acidic buffers can cause the cells to elongate at rates comparable to that induced by auxin (Rayle and Cleland 1992). The mediators of acid growth are believed to be a class of proteins called expansins (Cosgrove 1998). Besides expansins, some other agents that directly or indirectly enhance wall extensibility of growing cells can be endoglucanases, xyloglucan endotransglycosylase, etc. (Cosgrove 1999). Nevertheless, it has been suggested that physical rather than enzymatic processes are responsible for acid-enhancement of wall extensibility of isolated Characean wall materials (Métraux and Taiz 1977, 1979).

Stress relaxation in the walls of growing plant cells has been traditionally considered as either a creep or viscoelasticity based process (Probine and Preston 1962; Lockhart 1965a, b; Cleland 1967, 1971; Preston 1974; Taiz 1984). We have proposed a new model of wall stress relaxation (Wei and Lintilhac 2003), based on the assumption that any changes in cell turgor pressure, and in the resulting wall stress, must occur *gradually*. The model is based on the theory of *Loss of Stability*. The mathematics of *Loss of Stability* was originally developed by the great mathematician Leonhard Euler to model the behavior of columns in compression, and then extended by physicists to treat tensile stress relaxation (Rzhanitsyn 1955; Panovko and Gubanov 1965). In contrast to viscoelasticity and

creep, the prerequisite for *Loss of Stability* is that the load increases *gradually* until it reaches the critical value determined by material properties and wall geometry. The mathematics of *Loss of Stability* applies with equal validity to any thin-walled pressure vessel. As the internal pressure and the resulting stress in the wall *gradually* increase to the critical values, *Loss of Stability* must occur, leading to stress relaxation in the wall.

It is significant that *Loss of Stability* theory is derived from physical first principles rather than having been selected from a number of alternatives as a “best fit” to experimental observations. Thus we can say that *Loss of Stability* is an inevitable result of gradually increasing load. When stress relaxation in the walls of growing cells is treated as a manifestation of *Loss of Stability*, much of the puzzling behavior of cell walls can be explained (Wei and Lintilhac 2003). All of the previous studies on wall extensibility were conducted under creep or viscoelastic conditions. In contrast, the present study used ramp-loading conditions as required by *Loss of Stability*.

Materials and methods

Cultures of *C. corallina* were grown in a medium of 5% soil mixture in distilled water. Cell wall materials for mechanical testing were obtained from internodes that had reached about one-third of their mature length. These internodal cells were opened with a razor blade and the cytoplasm was removed with a hair loop. The test specimens took the form of a rectangular wall ribbon which was obtained by cutting the wall material with a pair of evenly spaced razor blades set at the desired angle to the cell axis. Typical ribbon widths were between 1.0 and 1.2 mm; the length varied according to the orientation of the ribbon with respect to the cell axis. To facilitate the mechanical testing of transverse ribbons (for a cell of 0.5 mm radius, the length of transverse ribbon was 3.1 mm), we developed a method whereby a short wall ribbon could be glued (ethyl cyanoacrylate adhesive) at its ends to a plastic substrate which was then mounted on the testing frame. Care was taken to ensure that the wall ribbon was kept wet during the preparation.

The original length (not including the glue line) and width of the wall ribbons were measured with an optical micrometer. Wall thickness was measured by means of image duplicating interference microscopy according to Mach-Zender (Aus Jena, Peraval, see Preston 1974). For the calculation of the optical path difference we assumed the refractive index of the wall materials to be 1.55 (Preston 1974). These original dimensions of the wall ribbons are necessary for the calculation of stress and strain.

During the experiments the tested wall ribbon was immersed either in water (pH = 7.0) or in acid medium containing 1 mM citrate/phosphate buffer. The pH of

the buffer ranged from 6.0 to 3.5. Immersion of wall ribbons began as soon as the tested ribbon was glued on the loading assembly, and the experiment was initiated about 5 min later.

Two kinds of tensile loading experiments were conducted in the present study: the first involved the continuous stretching of wall ribbons with a load whose value was first gradually increased from zero, and then held constant at the final value. The second involved the cyclic loading and unloading of the wall ribbons within their elastic ranges. The former experiment was designed to establish the prolonged extension characteristics of wall ribbons when a constant load was applied under *Loss of Stability* conditions (see [Discussion](#)); whereas the latter was to obtain the stress-strain relationships of individual wall ribbons for the calculation of the elastic moduli. To obtain reliable modulus values, wall ribbons employed in the loading and unloading experiment were first subjected to the continuous stretching experiment. This was important for low pH experiments because the period of prolonged extension was necessary to precondition the ribbon, making it possible to derive a consistent slope for the determination of modulus.

All of the loading experiments were done using a commercial version of a mechanical testing frame previously developed in this laboratory (Vitrodyne V-200, Liveco Inc., Burlington, VT). This instrument incorporates a microprocessor based feedback control system capable of operating either in strain-controlled or load-controlled mode. Details of this device have been described elsewhere (Wei et al. 2001). For the continuous stretching experiment, the Vitrodyne was programmed to increase the tensile load from zero to a certain value, F_K , in about 5 min, and then maintain the load at that level for at least 40 min. The value of F_K was pre-estimated so that the stress in the wall ribbon would be comparable to that of the original cell at a physiologically reasonable turgor pressure of 0.5 MPa. The choice of ramping time is significant. Too short a time approaches the sudden load implied by creep conditions, whereas too long a time is simply inconvenient. We chose a ramp time of 5 min because it was sufficient to establish *Loss of Stability* conditions as confirmed by our stress-relaxation studies (see [Discussion](#)). For the cyclic loading and unloading experiment, the Vitrodyne was programmed to gradually increase the tensile load to a level, F_M , and then gradually reduce it to the initial value in about 1×10^{-3} N increments. In addition, we always set $F_M \leq F_K$ to avoid substantial prolonged extension thereby obtaining a reliable modulus value (see [Discussion](#)).

Elastic modulus was calculated from the results of the loading and unloading experiment, which we plotted as wall elongation versus tensile force (Fig. 1). The slope of the linear regression of data points in this plot, ξ , represents the elongation of the wall ribbon per unit change in load. In other words, if we assumed that the stress was due to one unit of load on the cross sectional area of the wall ribbon, the elongation was then equivalent to the

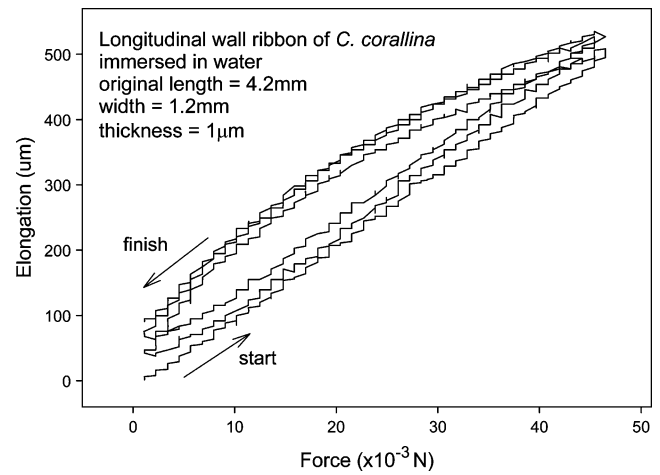


Fig. 1 Typical loading and unloading paths of stretching experiments conducted on longitudinal wall ribbons of growing *Chara corallina* cells. The tensile loading was applied by increasing the force in about 1×10^{-3} N increments to about 47×10^{-3} N and then reducing it to the initial value. Each loading and unloading cycle lasted about 10 min

value of the slope ξ . Hence we have the following equations for calculating the stress σ , strain ε , and elastic modulus E .

$$\sigma = \frac{I}{wt}, \quad (1)$$

$$\varepsilon = \frac{\xi}{l}, \quad (2)$$

$$E = \frac{\sigma}{\varepsilon} = \frac{l}{\xi wt}, \quad (3)$$

where l is unit force; w , t and l represent the width, thickness, and the length of the ribbon, respectively.

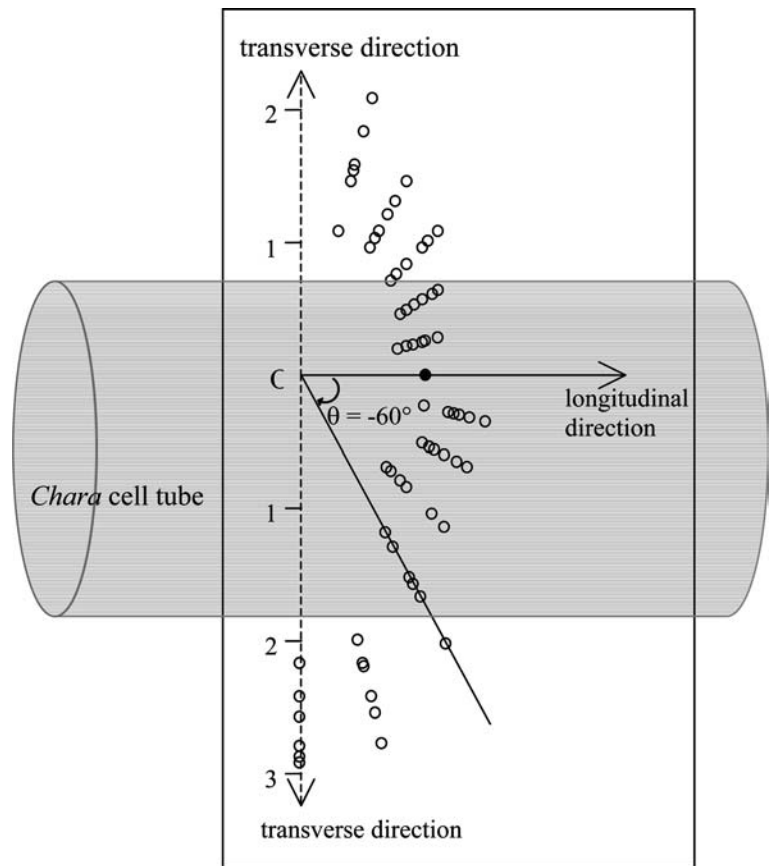
Results

Cell wall materials immersed in water

Figure 1 shows typical loading and unloading paths of a longitudinal wall ribbon immersed in water. The loading and unloading paths of other wall ribbons had a similar pattern, but may have had different slopes. The r^2 of data points in the remaining loading and unloading cycles consistently ranged from 0.90 to 0.95.

Figure 2 shows the anisotropic modulus of wall materials immersed in water. This figure is presented in polar coordinates with the polar axis ($\theta = 0^\circ$) being the longitudinal direction of the cell ($\theta = 90^\circ$ represents transverse direction of the cell). Data were based on the modulus values obtained from six separate cells. In order to compare the degree of anisotropy of different cells, and because the variation in longitudinal modulus was minimal (311 ± 29 MPa), the longitudinal modulus of all cells was normalized to 1 (indicated as the solid circle at $\theta = 0^\circ$). Thus the distance between the polar

Fig. 2 The anisotropic modulus of *C. corallina* cell walls presented in polar coordinates (the outer wall surface up). The angle θ follows the convention for left-handed anisotropy ($\theta=0^\circ$ and $\theta=90^\circ$ represent longitudinal and transverse azimuths of the cell, respectively). Data were based on six cell measurements. In order to compare the degree of anisotropy of different cells, the longitudinal modulus of all cells was normalized to 1 (indicated as the solid circle at $\theta=0^\circ$). Thus the distance between the polar origin (O) and any point on the graph stands for the relative value of the modulus along the azimuth θ . (Note: the longitudinal modulus = 311 ± 29 MPa)



origin, O , and any point on the graph stands for the relative value of the modulus along the azimuth θ .

Cell wall materials immersed in acidic buffer

Figure 3 shows the characteristic effect of acid pH on wall extensibility. This figure shows the percent elongation of longitudinal wall ribbons when tensioned in different solutions. Although the orientation of the wall ribbons was longitudinal in this example, other azimuthal orientations showed similar overall extension characteristics in buffers of varying pH. The five wall ribbons we tested had the same dimensions and were excised longitudinally from the same cell. During the first 5 min, the load was increased linearly from zero to 0.1 N, and then kept at this level for 40 min.

In pH=6 buffer, the cyclic loading/unloading paths of the wall ribbons were similar to those seen in water (i.e., Fig. 1). However, the paths of wall ribbons immersed in solutions of lower pH were very different. The main characteristic of the pattern was that, if the ribbon did not undergo pre-tension, the cyclic paths showed continuous upward drift (Fig. 4). The lower the pH, the more pronounced the drift. On the other hand, for wall ribbons that had been pre-tensioned with the continuous stretching experiment, the upward drift of the paths could be reduced considerably. Note that the maximum

load during cyclic loading/unloading was set to be equal to or less than the constant force in the stretching experiment, i.e., $F_M \leq F_K$. If loaded beyond F_K , the cyclic paths would continue to drift upward.

Table 1 shows the values of wall modulus calculated via Eqs. 1 \rightarrow 3. It is evident that acid pH has lowered

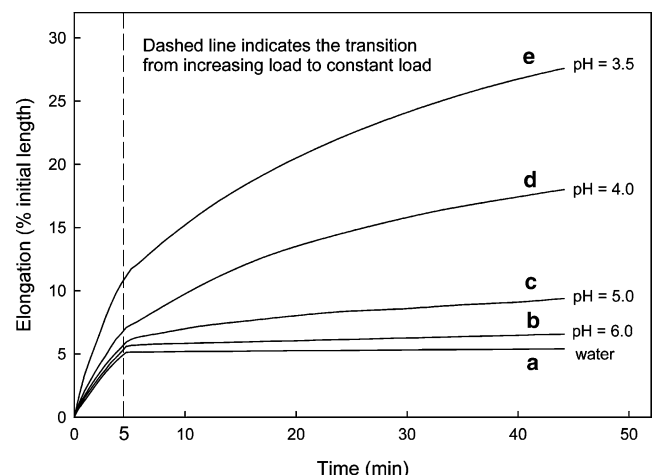


Fig. 3 Effects of acid pH on the extensibility of wall ribbon. In the first 5 min the load was linearly increased from zero to 0.1 N, and then was kept constant for another 40 min. All wall ribbons were excised longitudinally from a growing *Chara* internodal cell, and had the same dimensions (length, width, and thickness were 5.0, 1.2 mm, and 1.2 μ m, respectively)

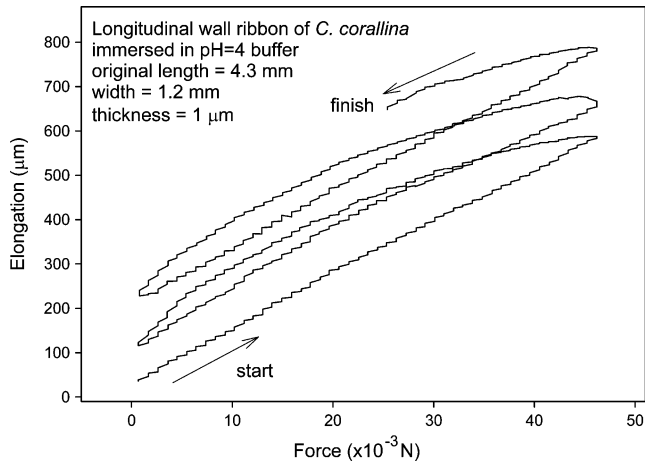


Fig. 4 The loading and unloading paths of a longitudinal wall ribbon immersed in 1 mM acidic buffer (pH=4). Different from that of Fig. 1, a significant plastic deformation occurred after the cyclic tensile load returned to zero

the modulus values; especially when pH=4.0. The statistics in the table were based on the results of wall ribbons obtained from six different cells. (Note: we were not able to calculate the moduli of wall ribbons in pH=3.5, since the loading/unloading paths had significant upward drift).

Figure 5 shows the nonlinear regression lines of the data points presented in Table 1, and graphically illustrates the relationship between anisotropic modulus and

the effect of acid pH. The regression equation employed was the “exponential linear combination” $y = y_0 + ae^{-bx} + cx$, where y_0 , a , b and c were parameters determined by the original data.

Discussion

The prolonged extension of wall ribbons; creep and *Loss of Stability* conditions

Many classic studies have used excised wall materials from the Characean algae *Nitella* and *Chara* as models for the study of cell wall elasticity and the effects of acid pH, however almost all of the experiments were conducted under creep or viscoelastic conditions. This is not surprising, since stress relaxation in plant cell walls has been traditionally considered as either a creep or viscoelasticity based process. We have suggested recently that *Loss of Stability* more correctly describes the mechanism of wall stress relaxation (Wei and Lintilhac 2003). One of the distinctions between creep and *Loss of Stability* is the way in which tensile force is loaded on the materials. In creep, a constant load, using whatever method, is suddenly loaded onto the test materials; whereas in *Loss of Stability*, load is gradually increased. This distinction not only reflects very different assumptions regarding the mechanism of stress relaxation but also potentially leads to very different views of the underlying controls of plant cell growth in general. Stress in the walls of living

Table 1 The modulus values of the wall ribbons immersed in water and in acidic buffers

Azimuth angle (degree)	Modulus (MPa) (in water)	Modulus (MPa) (in pH = 6.0)	Modulus (MPa) (in pH = 5.0)	Modulus (MPa) (in pH = 4.0)
-90°	808 ± 130	781 ± 132	750 ± 119	680 ± 136
-75°	783 ± 102	745 ± 129	694 ± 110	652 ± 103
-60°	550 ± 69	539 ± 64	512 ± 63	488 ± 52
-45°	413 ± 45	360 ± 37	351 ± 44	313 ± 42
-30°	401 ± 74	379 ± 67	356 ± 59	315 ± 63
-15°	398 ± 66	398 ± 72	352 ± 53	312 ± 65
0°	311 ± 29	312 ± 26	282 ± 30	241 ± 37
15°	291 ± 49	284 ± 42	265 ± 36	213 ± 25
30°	337 ± 37	334 ± 46	300 ± 44	259 ± 36
45°	374 ± 62	380 ± 61	347 ± 78	313 ± 62
60°	425 ± 80	412 ± 68	383 ± 80	329 ± 65
75°	517 ± 112	513 ± 83	499 ± 88	450 ± 86

Data are expressed in mean value ± standard deviation ($n=6$). Wall ribbons were obtained by cutting the wall materials along different azimuths from -90 to $+75^\circ$ in 15° intervals. The azimuth angle follows the convention for left-handed anisotropy ($\theta=0^\circ$ represents longitudinal θ direction; -90° represents transverse direction of the cell)

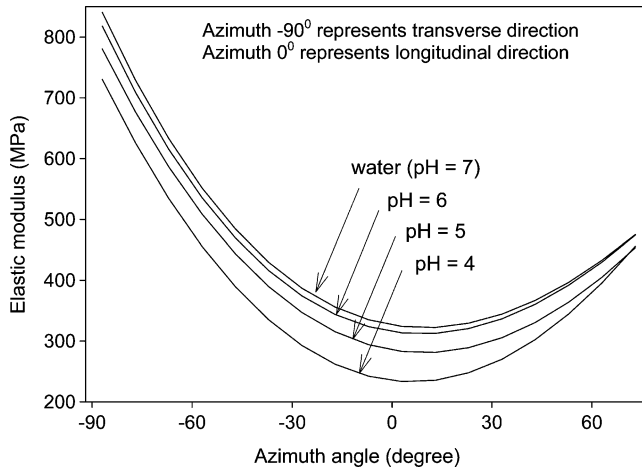


Fig. 5 Non-linear regression curves representing the effect of acid pH on anisotropic elastic modulus of growing *Chara* cell walls (see text)

cells arises from cell turgor pressure, which of course cannot jump suddenly from zero to the fully turgid state. Therefore the sudden loading implied by the creep model clearly does not reflect in vivo growth conditions. *Loss of Stability* loading however, is faithful to real growth conditions since cell turgor pressure and the resulting wall stresses increase gradually.

The aims of the present study are to first investigate the extensibility of the wall ribbons under ramp-loading conditions similar to those required by *Loss of Stability*, and second to obtain multi-azimuthal descriptions of the anisotropic elastic modulus of the walls. In the continuous stretching experiment the constant force, F_K , loaded onto the wall ribbon was increased gradually from zero in conformity with the requirements of *Loss of Stability* theory. The value of F_K was pre-calculated so that the stress in the tested wall ribbon would be close to that experienced by the original cell wall at 0.5 MPa cell turgor pressure. For a longitudinal wall ribbon,

$$\sigma_K = \frac{F_K}{wt}, \quad (4)$$

$$\sigma_L = \frac{PR}{2t}. \quad (5)$$

Equation 4 calculates the stress in the wall ribbon, σ_K . By definition it equals the tensile force F_K divided by the product of ribbon width w and wall thickness t . Equation 5 relates the longitudinal wall stress of a cylindrical pressure vessel σ_L to the pressure P , the radius R and the wall thickness t of the cylinder. Accordingly, the load applied to a transverse wall ribbon should be twice that for a longitudinal ribbon of the same cross sectional area. For oblique wall ribbons, of course, F_K should be set at an intermediate value.

For the experiments described in Fig. 3, five wall ribbons were excised from the same cell, at the same azimuth (longitudinal), and had the same dimensions. Moreover, the forces loaded onto the ribbons were also

the same. Therefore Fig. 3 is a direct comparison of the effects of different pH. As shown in the figure, acid pH did enhance wall extensibility, but the effect became substantial only when $\text{pH} \leq 4.0$. The dramatic enhancement of extensibility is seen not only in the separation of the curves, but also showed up in the rate of the prolonged extension (slope) under constant load. After the load stopped increasing, the curve of $\text{pH} = 6$ continued horizontally at essentially zero slope. At low pH however, as shown by the curves representing $\text{pH} = 4.0$ and $\text{pH} = 3.5$, the wall ribbons showed significant prolonged extension.

The acid-induced wall extensibility discussed above is significantly different from those noted in earlier studies. For instance, it has been reported that *Nitella* walls immersed in acid pH showed a linear relationship between wall extension and the logarithm of time under creep conditions (Métraux and Taiz 1977). However, we find no log-linear relationship when we re-plotted the last 40 min of the curves in Fig. 3. In comparing this experiment with that of Métraux and Taiz (1977), the acid pH and the wall stresses in the two experiments were comparable, but the results were very different. In their experiments, isolated *Nitella* wall tubes perfused with $\text{pH} = 6$ citrate/phosphate buffer were suddenly loaded with a weight W . Fourteen minutes later the pH was changed from 6 to 3.5. The time-course of extension was continuously recorded for the duration of the experiment. In both experiments the load-induced stress intensities were pre-calculated to be equivalent to a turgor pressure of 0.5 MPa. Why is it that with the same experimental materials, the same medium pH, and the same stress intensities, the log-linear relationship which they noted is not seen in our result?

We believe that both of the outcomes are legitimate considering the respective experimental conditions under which they were obtained, although only one is relevant to growth conditions. In the experiment carried out by Métraux and Taiz (1977), the weight W was loaded onto the wall materials suddenly, in contrast, our F_K was gradually increased from zero in about 5 min. This reflects the distinction between the paradigms under which the two experiments were conducted. Under creep conditions, stress is not initially evenly distributed along the tested materials, and the creep process is in itself a process of stress relaxation along the length of the materials. In Panovko's words, "creep produces a gradual redistribution of stresses in statically indeterminate system" (direct quote from Panovko and Gubanova 1965). In contrast, under ideal *Loss of Stability* conditions the load is slowly increased, so that the equilibrium state within the tested materials can keep up with the increasing stress. It is for this reason that if the load keeps increasing gradually until it reaches a critical value, the system can attain a metastable condition between stable and unstable states (and hence the transition from one to the other is termed "loss of stability") (Wei and Lintilhac 2003). In mathematical terms, these

conditions are met when the slope of the load-elongation relationship approaches zero.

By looking into whether or not changes in strain can keep up with changes in load, we can better understand the importance of loading rate in the experiment. In Fig. 3, curve *a* is virtually horizontal immediately following the switch from ramp-loading to constant load, implying that the changes in the strain are able to keep up with the increasing stress intensities acting through the sample. This suggests that for wall ribbons immersed in water, the rate of increasing the load from zero to 0.1 N within 5 min is slow enough to establish *Loss of Stability* loading conditions. If the 0.1 N load had been applied to the wall ribbon *suddenly*, one would expect the resulting curve to be very different. Indeed, Probine and Preston (1962) reported that the creep behavior of *Nitella* wall ribbons showed a consistent pattern: the strain changes were large immediately following load application, and were still observable after 16 h. Furthermore, the relationship between strain and log time was also linear, as were those found by Métraux and Taiz (1977) with wall ribbons immersed in acid environments.

Probine and Preston (1962) also did a thoughtful replotting in their analysis of the effect of load magnitude on creep; they arbitrarily adjusted the wall extension to zero at 1 min and re-plotted the curves. Their re-plottings clearly show that the rate of extension increased dramatically as the load magnitude increased, with no suggestion that a limiting extension had been reached. We have reason to believe that this is typical behavior for any creep-based experiment, and confirms the *power law* relationship suggested by Panovko and Gubanova (1965) in their book *Stability and Oscillations of Elastic Systems*. They stated that, “In making a theoretical solution of any problem in loading of a structure with creep, it is necessary to know the creep law—the relation between the acting force σ and the creep rate $\dot{\epsilon}_C$,

$$\dot{\epsilon}_C = \left(\frac{\sigma}{\lambda}\right)^m, \quad (6)$$

where λ and m are constants of the material.” (direct quote from Panovko and Gubanova 1965). The power law, Eq. 6, clarifies the observation that the relationship between extension rate and load magnitude is exponential under creep conditions, which directly explains Probine and Preston’s replotted curves.

It is clear from Fig. 3 that the lower the pH, the greater the slope of the time-course extension curves. The enhancement of wall extensibility at $\text{pH} \leq 4.0$ explains why the cyclic loading/unloading paths in Fig. 4 continuously drift upward, building up a considerable plastic deformation. For that reason, to obtain a reliable stress-strain relationship (the slope ζ in Eq. 3) for calculating wall moduli, wall ribbons employed in cyclic loading/unloading experiment were first subjected to the continuous stretching experiment. In addition, the maximum force level of the loading/unloading cycle, F_M ,

did not exceed the constant force in the continuous stretching experiment, F_K (i.e., $F_M \leq F_K$).

For loading/unloading experiments conducted in water, the purpose of preconditioning wall ribbons via the continuous stretching experiment was to eliminate the variation of the first loading path. Without preconditioning, the first loading path of Fig. 1 differs significantly from all subsequent loading and unloading cycles (see Wei and Lintilhac 2003). Although this may be due in part to the rupture of encrusting materials on the outer surface of the cell or the straightening of polymeric materials within the wall, the phenomenon is indeed typical in this kind of mechanical testing. In engineering terms the irrecoverable elongation generated by the first loading path is referred to as *residual strain*, which reveals the *plastic strain* component caused by the relevant maximum load. Despite the fact that it is denoted as *plastic* strain, the tested material can still show complete elastic recovery in the subsequent loading and unloading cycles, as long as the load does not exceed the maximum value (Chen and Han 1987).

As indicated in Table 1, the ratio of transverse/longitudinal modulus for ribbons immersed in a water medium ($\text{pH} = 7.0$) was 2.60; whereas this ratio became 2.82 when the medium was buffered to $\text{pH} = 4.0$. This coincides with the Acid Growth Theory, as a higher value of the ratio favors cell elongation. It has been suggested that low pH may directly weaken the H-bonding between the xyloglucan matrix and the cellulose component, thereby permitting microfibril slippage (Keegstra et al. 1973). Keegstra’s proposal may also explain the increase in the ratio of the two moduli at low pH because ribbons oriented longitudinally are significantly longer than those oriented transversely, and therefore they also may exhibit greater inter-microfibrillar slippage.

Anisotropic elasticity and cylindrical growth

In the context of growth morphologies, we can now turn our attention to how the cylindrical growth habit is maintained by an overall anisotropy in the longitudinal and transverse directions. Because *Chara* cells legitimately qualify as thin-walled cylinders, there must be a 1:2 longitudinal to transverse stress ratio on the side walls, i.e., transverse wall stress σ_T must be twice the longitudinal wall stress σ_L (Lockhart 1965b):

$$\sigma_T = 2\sigma_L = \frac{PR}{t}, \quad (7)$$

where P is turgor pressure, R and t are the radius and wall thickness of the cell, respectively. How then can these cells continue to grow longitudinally when the transverse stress is necessarily twice the longitudinal stress? Table 1 shows that for *Chara* cells of this developmental stage, the transverse modulus E_T is larger than longitudinal modulus E_L by a ratio of 2.60 (ranges from

2.21 to 2.87). Thus we see that the geometrically mandated lower stress in the longitudinal direction is compensated for by the increased stretchiness in that direction, making it possible for the cell to maintain the cylindrical growth habit. Note that variation in longitudinal modulus is minimal (Table 1, $\theta=0^\circ$). In contrast, transverse modulus is more variable than that of other directions (Table 1, $\theta=-90^\circ$), probably because the transverse ribbon was the shortest, and the error caused by irregularities at the glue line more significant.

Figure 2 shows that the lowest modulus is along $\theta=15^\circ$, which means that the principal longitudinal mechanical axis does not align precisely with the cell's longitudinal geometrical axis. Correspondingly, the second (transverse) mechanical axis does not align with cell's transverse direction. Thus the deviation of the two principal axes (X' and Y') relative to the cell's geometrical axes (X and Y) can be sketched as Fig. 6. The third axis (Z) is not shown in the figure. It corresponds to the radial direction, i.e., perpendicular to the plane of the wall surface.

The effect of this deviation of the principle mechanical axes from the geometrical axes can be understood as follows. If we open a cylinder made of similarly deviated anisotropic material lengthwise we will initially obtain a right-rectangle of wall material. But, noting that any expansion in wall materials that have off-axis anisotropy will lead to transverse shear (Love 1927), we see that if we stretch the rectangle uniformly in all directions the linear stress-strain relationship will result in the deformation of the rectangle into a parallelogram. If we now roll it into a cylinder again, one end will have twisted with respect to the other.

It is well known that many free-standing cylindrical cells exhibit the phenomenon of twisting growth, i.e., as the cells grow in length they also twist about their own axes (Green 1954; Castle 1942). Probine (1963) suggested that this spiral growth phenomenon was due to orthorhombic elastic symmetry of the cell walls. Now,

with a clear picture of wall anisotropic elasticity, the spiral growth phenomenon can be easily understood.

Theoretical studies of wall anisotropy are commonly pursued within the framework of stress-strain analysis, focusing in particular on cylindrical cell models because many types of plant cells may be regarded as the compression forms of thin-walled cylindrical pressure vessels (Love 1927; Sellen 1980, 1982; Cowdey and Preston 1966). Sellen (1982) pointed out that if we assume orthorhombic symmetry and suppose that no stress is applied in the radial direction (as we are not interested in changes in wall thickness), the compliance and the stress-strain equation can be simplified considerably. Using Sellen's equations, the stress relationships of the walls of any cylindrical plant cells can be elucidated as follows. Under the coordinates shown in Fig. 6, the compliance S_{ik} (where i and k may take any values from 1 to 6) reflecting the walls' elastic anisotropy is originally a "6 by 6" matrix. As the relationships between stresses along the mechanical axes ($\sigma_{X'X'}$, $\sigma_{Y'Y'}$) and stresses along the cell's axes (σ_T , σ_L) are,

$$\sigma_{X'X'} = \sigma_T \cos^2 \theta + \sigma_L \sin^2 \theta, \quad (8)$$

$$\sigma_{Y'Y'} = \sigma_T \sin^2 \theta + \sigma_L \cos^2 \theta. \quad (9)$$

Substituting Eqs. 4 and 5, we have:

$$\sigma_{X'X'} = \frac{\text{Pr}}{t} \left(\cos^2 \theta + \frac{\sin^2 \theta}{2} \right), \quad (10)$$

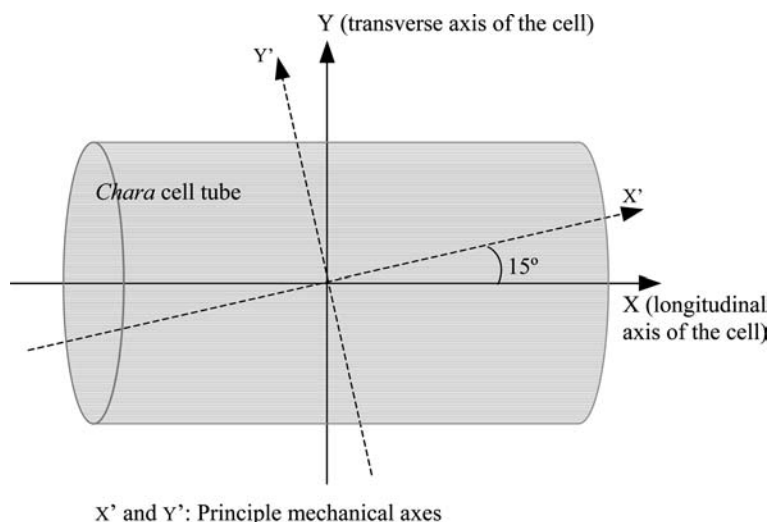
$$\sigma_{Y'Y'} = \frac{\text{Pr}}{t} \left(\sin^2 \theta + \frac{\cos^2 \theta}{2} \right). \quad (11)$$

Thus in general,

$$2\sigma_{Y'Y'} > \sigma_{X'X'}. \quad (12)$$

Comparing Eqs. 12 and 7 we can see that if $\theta=0$ (i.e., if the mechanical axes do not deviate from the cell's geometrical axes), Eq. 12 will be converted into Eq. 7. Conversely, a higher value for the deviation angle θ will

Fig. 6 The principle axes of mechanical symmetry (X' , Y') relative to the cell's geometrical axes (X , Y). According to our measurements, the principle mechanical axes deviate from the relevant cell's axes by about 15°



lead to higher degree of “inequality” in Eq. 12. Hence we see the connection between the offset of the axes and the general relationship between transverse and longitudinal stresses in the walls of cylindrical cells.

The critical role of microfibril orientation in determining cell shape has been demonstrated by Green (1968) and his colleagues. They used microtubule toxins such as colchicine and isopropyl-phenylcarbamate (IPC) to randomize the deposition of microfibrils. Such cells tend to grow as spheres rather than as cylinders. There is also direct evidence that mechanical anisotropy reflects an underlying structural anisotropy, and that when there is a preferred orientation of the cellulose fibrils, the cell wall is reinforced in that direction (Kerstens et al. 2001). However, we still lack detailed information about the relationship between the principle mechanical and geometrical axes, and the orientation of microfibrils in the walls.

Conclusions

The prolonged extension characteristic of excised Characean wall materials under ramp-loading conditions is different from that seen under creep conditions. Where a linear relationship between wall extension and log time is typical for creep-based experiments, it is not seen under ramp-loading conditions. This reflects the distinction between two stress relaxation mechanisms, creep and *Loss of Stability*.

Acid pH enhances the extensibility of the wall materials, especially when medium $\text{pH} \leq 4.0$. Under ramp-loading conditions, this acid enhancement is not only evident in the separation of the curves seen in Fig. 3, but also in the slope of the prolonged extension curves. This means that to obtain meaningful modulus values of wall materials immersed in acid environments, elimination of the prolonged plastic extension induced under acid conditions is necessary. Acid pH may also further enhance the anisotropy of the wall modulus. For instance, pH 4.0 increases the ratio of transverse/longitudinal modulus from 2.60 to 2.82.

Anisotropic elasticity is central to the problem of understanding cylindrical growth in that the transverse modulus must be greater than the longitudinal modulus. Furthermore, in order to produce twisting growth the principal longitudinal mechanical axis must deviate from the cell's longitudinal geometrical axis by some significant amount.

The marriage of the concept of *Loss of Stability* with a more detailed description of wall anisotropy promises to provide a reasonable basis for understanding the cylindrical growth habit in Characean cells. The extent to which these mechanisms can be applied to higher plant growth remains to be seen. However the same physical principles governing wall extensibility and cell enlargement must be at work. We anticipate that a better understanding of the nature of *Loss of Stability* conditions, as modified by local structural and multi-

cellular constraints, biochemical tuning of the system and other metabolic inputs, will lead in turn to a better understanding of growth behavior in multicellular plant organs in general.

Acknowledgement We would like to thank Dr. Jean-Guy Beliveau, Department of Civil and Environmental Engineering, The University of Vermont, for his thoughtful reading of this manuscript.

References

- Castle ES (1942) Spiral growth and reversal of spiraling in *Phycomyces* and their bearing on the primary wall structure. *Am J Bot* 29:664–684
- Chen WF, Han DJ (1987) *Plasticity for structural engineers*. Springer, Berlin Heidelberg New York
- Cleland RE (1967) Extensibility of isolated cell walls: measurement and changes during cell elongation. *Planta* 74:197–209
- Cleland RE (1971) Cell wall extension. *Annu Rev Plant Physiol* 22:197–222
- Cosgrove DJ (1998) Cell wall loosening by expansins. *Plant Physiol* 118:333–339
- Cosgrove DJ (1999) Enzymes and other agents that enhance cell wall extensibility. *Annu Rev Plant Physiol Plant Mol Biol* 50:391–417
- Cowdrey DR, Preston RD (1966) Elasticity and microfibrillar angle in the wood of Sitka spruce. *Proc R Soc B* 166:245–272
- Green PB (1954) The spiral growth pattern of the cell wall in *Nitella axillaries*. *Am J Bot* 41:403–409
- Green PB (1968) Cell morphogenesis. *Annu Rev Plant Physiol* 20:365–394
- Hager A, Menzle H, Krauss A (1971) Versuche und Hypothese zur Primärwirkung des Auxins beim Streckungswachstum. *Planta* 100:47–75
- Keegstra K, Talmadge KW, Bauer WD, Albersheim P (1973) The structure of plant cell walls. *Plant Physiol* 51:188–196
- Kerstens S, Decraemer WF, Verbelen JP (2001) Cell walls at the plant surface behave mechanically like fiber-reinforced composite materials. *Plant Physiol* 127:381–385
- Lockhart JA (1965a) An analysis of irreversible plant cell elongation. *J Theor Biol* 8:264–275
- Lockhart JA (1965b) Cell extension. In: Bonner JE, Varner JE (eds) *Plant biochemistry*, Academic, New York, pp 827–849
- Love AEH (1927) *Treatise on the mathematical theory of elasticity*. University Press, Cambridge
- Métraux JP, Taiz L (1977) Cell wall extension in *Nitella* as influenced by acids and ions. *Proc Nat Acad Sci* 74:1565–1569
- Métraux JP, Taiz L (1978) Transverse viscoelastic extension in *Nitella*. I. Relationship to growth rate. *Plant Physiol* 61:135–138
- Métraux JP, Taiz L (1979) Transverse viscoelastic extension in *Nitella*. II. Effect of acid and ions. *Plant Physiol* 63:657–659
- Métraux JP, Richmond PA, Taiz L (1980) Control of cell elongation in *Nitella* by endogenous cell wall pH gradients. *Plant Physiol* 65:204–210
- Panovko YG, Gubanov II (1965) *Stability and oscillations of elastic systems*. Consultants Bureau, New York
- Preston RD (1974) *The physical biology of plant cell walls*. Chapman & Hall, London
- Probine MD (1963) Cell growth and the structure and mechanical properties of the wall in the internodal cells of *Nitella opaca*. III. Spiral growth and wall structure. *J Exp Bot* 14:101–113
- Probine MC, Preston RD (1961) Cell growth and the structure and mechanical properties of the wall in internodal cells of *Nitella opaca*. I. Wall structure and growth. *J Exp Bot* 12:261–282
- Probine MC, Preston RD (1962) Cell growth and the structure and mechanical properties of the wall in internodal cells of *Nitella opaca*. II. Mechanical properties of the walls. *J Exp Bot* 13:111–127

- Rayle DL (1973) Auxin-induced hydrogen-ion excretion in *Avena* coleoptiles and its implications. *Planta* 114:63–73
- Rayle DL, Cleland RE (1970) Enhancement of wall loosening and elongation by acid solutions. *Plant Physiol* 46:250–253
- Rayle DL, Cleland RE (1992) The acid growth theory of auxin-induced cell elongation is alive and well. *Plant Physiol* 99:1271–1274
- Rzhanitsyn AR (1955) Stability of the equilibrium of elastic systems. Gostekhizdat, Moscow
- Sellen DB (1980) The mechanical properties of plant cell walls. In: Vincent JFV, Currey JD (eds) *The mechanical properties of biological materials*, (34th symposium of the society for experimental biology). Cambridge University Press, Cambridge, pp 315–329
- Sellen DB (1982) The response of mechanically anisotropic cylindrical cells to multiaxial stress. *J Exp Bot* 34:681–687
- Taiz L (1984) Plant cell expansion: regulation of cell wall mechanical properties. *Annu Rev Plant Physiol* 35:585–657
- Wei C, Lintilhac PM (2003) Loss of stability—a new model for stress relaxation in plant cell walls. *J Theor Biol* 224:305–312
- Wei C, Lintilhac PM, Tanguay JJ (2001) An insight into cell elasticity and load bearing ability: measurement and theory. *Plant Physiol* 126:1129–1138